

Validation of the CHEMISTRY Solver in LS-DYNA

Hamid Rokhy¹, Reza Nasouri², Arturo Montaya², Adolfo Matamoros², Roya Bakzadeh³

¹Department of Aerospace Engineering, Amir Kabir University of Technology, Tehran, Iran

²Department of Civil and Environmental Engineering, University of Texas at San Antonio, TX, U.S

³Department of Mining Engineering, Urmia University, Iran

Abstract

The CHEMISTRY solver has been added to the LS-DYNA software, enabling users to model and predict accidental gas explosions in refinery plants, pipelines, and coal mines. Although this new solver has shown theoretical potential in chemical, oil and gas refineries, there are limited studies implementing the capabilities provided by the CHEMISTRY solver. In this study, a series of fundamental chemistry problems were simulated, to compare the numerical results with existing experimental data. This study finds excellent agreement between solver results and experimental data, proving a high level of precision obtained through the CHEMISTRY solver.

1 Introduction

A large number of industrial problems relating to chemistry are in fluid structure interaction (FSI) forms. Some examples include the large plastic deformation of a tube due to an internal gas detonation [1-2], blast relief wall in offshore plants [3], blast wave propagation from gas mixture detonation [4] and sheet metal forming by gas detonation [5-6].

The complexities involved in the FSI problems make the calculation of analytical solutions very difficult or even impossible. Moreover, experimental tests are limited, dangerous and costly. Therefore, numerical methods are the preferred tools to examine these problems in the complex interaction between fluid flow with chemical reactions and solid structures. But simulation of these complex phenomena is a challenge for the fluid solver, chemistry solver, mechanical solver and the coupling algorithm.

Recently, the CESE-IBM FSI method with finite rate chemistry model in LS-DYNA® commercial code was added to handle these complex FSI problems. Although this new solver has shown valuable potentials in chemical, oil and gas refineries, there are limited studies implementing the capabilities provided in the CHEMISTRY solver. For this reason, a series of fundamental chemistry problems were simulated using this solver to compare the numerical results with existing experimental data. The present paper will discuss the results of these validations with a detailed chemistry model such as H_2/O_2 and C_3H_8/O_2 reactions.

2 CESE method with finite rate chemistry model

To evaluate the accuracy of the CESE solver with a finite-rate chemistry model in solving the chemical reaction in compressible flow, four benchmark cases are investigated, and numerical results are compared with the experimental data.

1. Simulation of pulse detonation engine (PDE)
2. Diffraction and re-initiation of detonations behind a backward-facing step
3. Detonation initiation by shock reflection from rectangular obstacles
4. Blast wave propagation from gas mixture detonation

2.1 Simulation of pulse detonation engine (PDE)

Pulse detonation engines use detonation waves that propagate through a premixed fuel-air mixture and produce large chamber pressures and thereby thrust. PDEs offer the potential for high performance because the rapid detonation process results in constant volume combustion with very high operating frequencies and combustor chamber pressures. PDEs are predicated to be very efficient and offer good thrust characteristics, from the low subsonic to the high supersonic flight regimes. PDEs also have the potential to operate at very high energy densities, allowing the use of simple and compact combustor designs [7].

The CHEMISTRY solver has been used to simulate a 1D pulse detonation engine. Detonation was initiated in a stoichiometric H₂-O₂ mixture at initial pressure of 1atm, temperature of 300K and an initial velocity of zero. Detonation was directly initiated at the closed end by specifying an energetic initiation region (5atm, 3000K). Geometry of the computational set-up is shown in Figure 1. The fluid domain is a 200mm*20mm rectangular region. Since this setup is considered a one-dimensional problem, only one element was considered in the thickness direction. Non-reflective boundary conditions are employed for all boundaries.

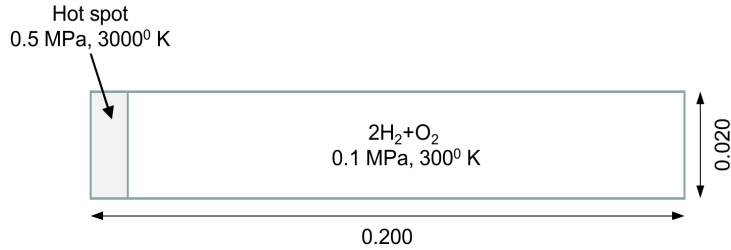


Fig. 1: The PDE model for numerical simulation

The detailed kinetic mechanism proposed by Liberman et al. [8], which consists of 8 chemical species (H₂, O₂, H, O, OH, H₂O, HO₂, and H₂O₂) and 9 reactions, was used for H₂-O₂ combustion. The reaction mechanism is presented in Table 1. We use the Liberman kinetic because it includes all the species in the H₂-O₂ detonation. In addition, this approach also reduces the computational time due to the lower number of reactions.

Reaction	Forward rate constant			Reverse rate constant		
	A	n	E	A	n	E
1 H ₂ +O ₂ =OH+OH	2.52E+12	0.00	39.0	1.16E+13	0.00	21.0
2 OH+H ₂ =H ₂ O+H	2.25E+13	0.00	5.24	9.90E+13	0.00	20.3
3 H+O ₂ =OH+O	1.55E+14	0.00	16.7	1.16E+13	0.00	0.705
4 H ₂ +O=OH+H	2.46E+13	0.00	9.84	1.07E+13	0.00	7.90
5 H+H+M=H ₂ +M	3.60E+15	0.00	0.0	1.46E+16	0.00	104.0
6 H+O ₂ +M=HO ₂ +M	3.60E+15	0.00	0.0	3.01E+15	0.00	47.8
7 HO ₂ +HO ₂ =H ₂ O ₂ +O ₂	1.00E+13	0.00	0.0	1.30E+14	0.00	40.0
8 OH+OH+M=H ₂ O ₂ +M	1.11E+16	0.00	1.92	7.40E+17	0.00	47.0
9 H+H ₂ O ₂ =H ₂ +HO ₂	1.17E+14	0.00	11.8	1.55E+14	0.00	28.5

Table 1: Detailed H₂-O₂ reaction mechanism, Units are cm³, mol, sec, kcal, K, and $k = A T^n \exp(-E/RT)$ [8]

Pressure change in the longitudinal direction for a few different times is shown in Figure 2. The detonation wave pressure estimated 19.5 bar, which is in great agreement with the experimental results [9]. Indeed, the detonation wave velocity in stoichiometric hydrogen-oxygen mixture is calculated as 2850 m/sec which also closely matches the experimental results reported by Moyle et al. in Ref. [9]. OH radical mass fraction change in the longitudinal direction for a few different times is shown in Figure 3. In fact, this figure represents the process of chemical reaction, because OH radical is the primary chain branching reaction in the hydrogen-oxygen combustion. Table 2, shows the present estimation of the mass fraction of all chemical species behind the detonation wave in comparison with those values reported by Moyle et al. in Ref. [9]. The small difference between the estimated values and the measured values relates to the kinetic mechanism that was chosen for the finite-rate chemistry model.

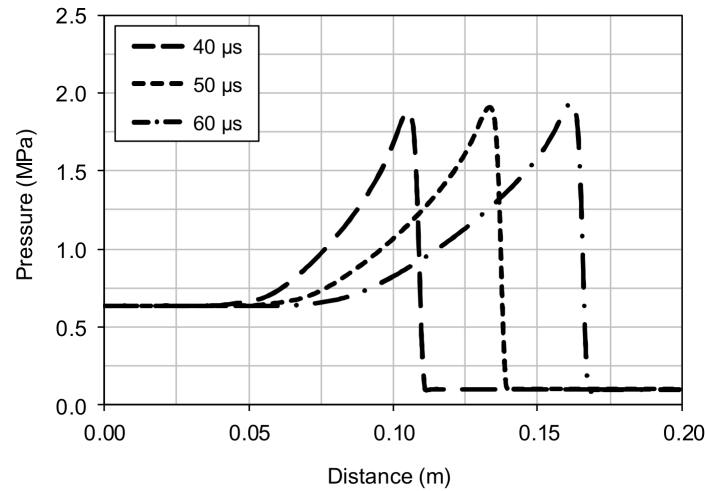


Fig. 2: Temporal evolution of pressure in the longitudinal direction

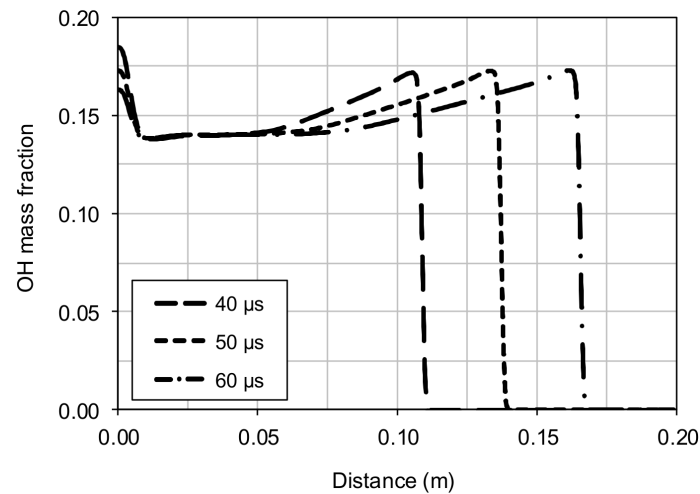


Fig. 3: Temporal evolution of OH mass fraction in the longitudinal direction

Species	Num.	Exp. [9]
H ₂	0.0253	0.0235
O ₂	0.1270	0.1107
H	0.0103	0.0052
O	0.0668	0.0719
OH	0.1591	0.1411
H ₂ O	0.6450	0.6476

Table 2: Mass fraction of the chemical species behind the detonation wave

2.2 Diffraction and re-initiation of detonations behind a backward-facing step

Diffraction of a shock wave behind a backward-facing step is one of the fundamental topics in shock wave dynamics. Rarefaction waves emitted from a diffraction corner reduce the strength of an incident shock wave. For detonation waves, although the situation is similar with the shock wave, the effects of the rarefaction waves are very complex and important for the combustion.

Diffraction phenomena of gaseous detonation waves behind a backward-facing step in a tube are investigated and numerical results are compared with experimental data [10]. Mixtures were stoichiometric H₂/O₂ non-diluted ($\beta = [\text{Ar}]/[\text{O}_2] = 0$) and diluted with argon ($\beta = 4$) at $P_0=26.7\text{kPa}$.

Figure 4 shows the computational setup of this problem. The chosen mesh size is 0.33mm. Solid wall boundary conditions were employed for boundaries except for left and right edges, where non-reflective boundary condition were applied.

Detonation of the mixture is accomplished by specifying a high energy initiation region. The pressure and temperature of this initiation region were considered 10 bar and 2500 K, respectively. These initial conditions guaranteed the explosion of the gas mixture and generated detonation wave in very short time before the backward-facing step. The H₂/O₂ combustion mechanism used here is the detailed mechanism proposed by Yungster [11]. This approach consists of 8+1 reaction species (H₂, O₂, H, O, OH, H₂O, HO₂, H₂O₂ and AR) and 19 reactions. This mechanism was selected due to the fact that it includes all of the crucial components existed in the hydrogen/oxygen reaction.

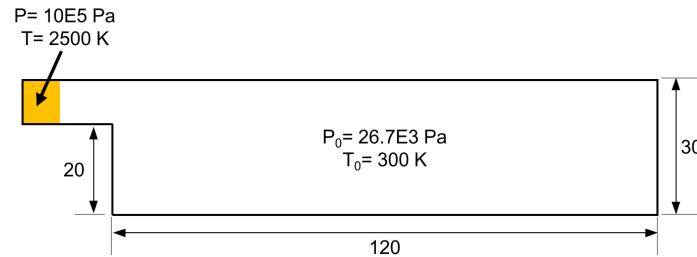


Fig.4: Geometry of computational set-up (all dimensions are millimeter)

Figure 5(a) shows the details of the pressure profile at the diffracted region just behind the step ($D = 0\text{mm}$). As can be seen, a weak shock of 5 times the initial pressure propagates first and is followed by a pressure wave of 10 times the initial pressure. The second wave is a reflected wave from the bottom wall. Figure 5(b) shows the profile at the distance $D = 65\text{mm}$ from the step. The steep pressure rise is higher than the CJ pressure ratio which indicates that the detonation wave is re-initiated. This graph demonstrated a good level of agreement between the numerical results and experimental data.

Figure 6 shows the contours of temperature during the diffraction of the detonation wave behind a backward-facing step. This figure provides a clear visual illustration for the re-initiation of the detonation wave in the process.

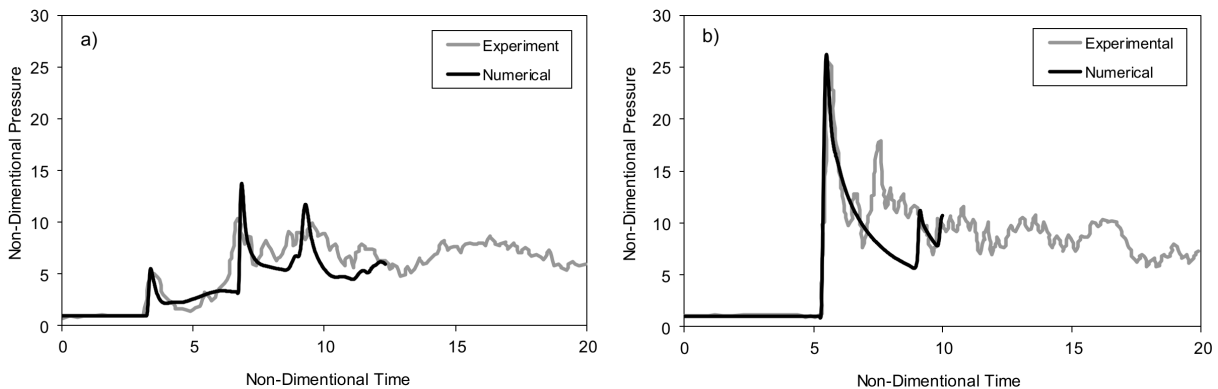


Fig.5: Pressure profiles behind the step for $\beta = 4$, $P_0 = 26.7\text{kPa}$; a $D = 0\text{mm}$, b $D = 65\text{mm}$

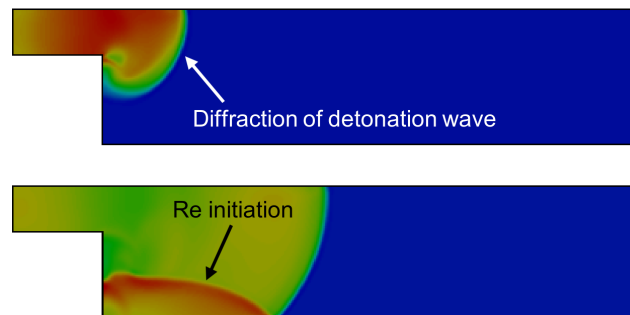


Fig.6: Contours of temperature behind the step for $\beta = 4$, $P_0 = 26.7\text{kPa}$

2.3 Detonation initiation by shock reflection from rectangular obstacles

To investigate the shock-induced combustion, ignition induced by the interaction of an initially planar shock wave with a single rectangular obstacle was studied, and the numerical results were compared

with the experimental data provided in [12]. In the case of a 2H₂+O₂+80%AR mixture, a planar incident shock wave with M_s=2.48 interacts as an obstacle. According to planner shock wave theory, pressure, temperature, and density behind the shock can be calculated as follows [13]:

$$\frac{P_2}{P_1} = \frac{2\gamma}{\gamma+1} M_1^2 - \frac{\gamma-1}{\gamma+1} \quad (1)$$

$$\frac{T_2}{T_1} = \frac{\left(1 + \frac{\gamma-1}{2} M_1^2\right) \left(\frac{2\gamma}{\gamma-1} M_1^2 - 1\right)}{\left[\frac{(\gamma+1)^2}{2(\gamma-1)}\right] M_1^2} \quad (2)$$

$$\frac{\rho_2}{\rho_1} = \frac{(\gamma+1) M_1^2}{(\gamma-1) M_1^2 + 2} \quad (3)$$

where P_1 , T_1 and ρ_1 are pressure, temperature and density of gas; M_1 is the Mach number of incident shock wave. Here, P_2 , T_2 and ρ_2 stand for the pressure, temperature and density behind the incident shock wave. The particle velocity of shock wave is calculated as follows [13]:

$$u_p = M_1 a_1 \left(1 - \frac{\rho_1}{\rho_2}\right) \quad (4)$$

In the above formula a_1 is the sound speed in the gas mixture and u_p is the particle velocity of shock wave. For the 2H₂+O₂+80%AR mixture, gamma is 1.589 and R is 241.8. By using the planner shock wave theory, we can easily compute the post-shock condition. This condition applied on the left side of the numerical model shown in Figure 7. The pre and post-shock conditions are shown in Table 3. The mesh size of the fluid is 0.4mm.

	P (KPa)	T (K)	u (m/s)
pre-shock	5300	300	0
post-shock	39450	784	551

Table 3: Pre and post shock condition

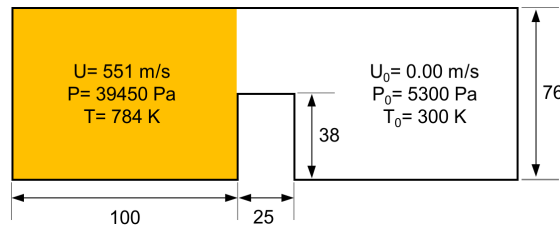


Fig.7: Geometry of computational set-up (all dimensions are millimeter)

In the hydrogen/oxygen combustion, there are two chemical reactions that have very large effect on determining ignition delay times ($H+O_2=OH+O$ and $H+O_2 (+M) =HO_2 (+M)$). These two reactions compete and greatly influence the amount of the OH radical begins produced. A small change in these two rates can have a large effect on the mechanism properties. Therefore, choosing an appropriate kinetic will be a great challenge in simulating such problems.

In this case, an 8+1 species and 21 reactions mechanism taken from Connaire et al. [14] has been used. Figure 8 shows the sequence of schlieren images of shock wave reflection and detonation front growth in this mixture. These results show that the CHEMISTRY solver predict shock diffraction and detonation initiation in this mixture with high accuracy. But our investigation shows that this accuracy is very dependent on the chemical kinetic chosen for hydrogen/oxygen combustion. Other detailed kinetic, such as CALTECH (8+1 species and 20 reactions) [15] and Yungster et al. (8+1 species and 19 reactions) [11] cannot predict this phenomenon well.

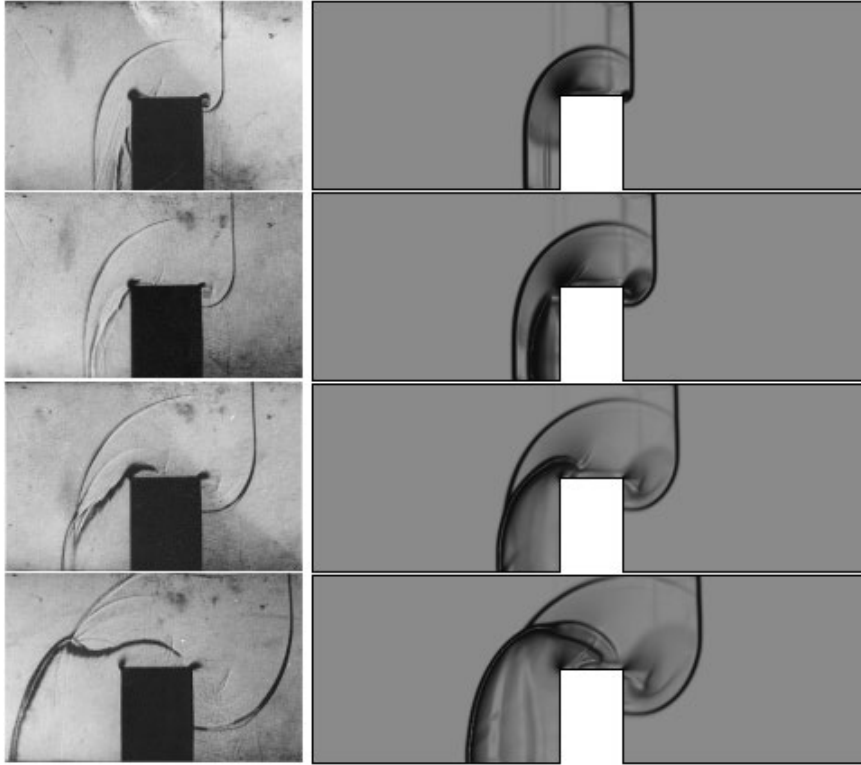


Fig.8: Sequence of schlieren images of shock wave reflection and detonation front growth with $2H_2+O_2+80\%AR$ ($M_s=2.48$, $P_1=5.26$ KPa). Left: experimental [12], Right: present study

2.4 Blast wave propagation from gas mixture detonation

To evaluate the accuracy of the kinetic mechanism and the validity of the simulation of the volumetric explosions, including the blast wave propagation and its interaction with the walls, the explosion of a certain volume of stoichiometric propane/oxygen mixture in a semi-confined volume is investigated, and the numerical results are compared with the experimental data [16]. The semi-confined volume consists of four walls, while the ceiling is open. The height of the walls is 250mm. The gas mixture, which is a 66 mm diameter hemispherical volume, explodes using a very strong electric spark. In the test performed, the effect of the walls on the amount of pressure recorded at three points was measured experimentally. Figure 9 shows the dimension of the geometry of the experimental study. Validation is performed for the case where only the first to third walls are present.

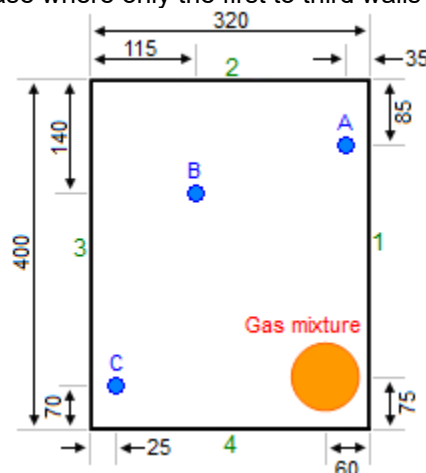


Fig.9: Experimental configuration [16] (all dimensions are millimeter)

The initial pressure and temperature of the mixture were 1 bar and 298 K, respectively. Detonation of the mixture is accomplished by specifying a high-energy initiation region. This region is considered as a hemispherical shape, containing hot combustion products (e.g., carbon dioxide and water vapor).

The pressure and temperature of this initiation region are considered to 3 bar and 3000 K, respectively. These initial conditions guarantee the explosion of the gas mixture.

Fig. 10 shows the 3D geometry of the computational set-up. As shown in Figure 10, the size of the elements near the rigid surface selected is equal to the desired value, while as the distance from the ground increases, their size increases by a certain ratio. Using this meshing method, it is possible to use a smaller element size to simulate the problem in the area close to the ground (where the sensors and the gas mixture are located) without significantly increasing the total size of the model elements. Due to hardware limitations available to the authors, the element size of 2mm was chosen for the fluid domain. Also, the walls have been applied with rigid wall conditions in the model, while outflow condition was applied for the other boundaries. The reduced kinetic mechanism proposed by Mawid et al. [17], which consist of 15 chemical species and 14 reactions, was used for $C_3H_8-O_2$ combustion. The reaction mechanism is presented in Table 4. We used this reduced kinetic because it includes all of the important species in the $C_3H_8-O_2$ detonation and on the other hand, it reduces the computational time due to the lower number of chemical species and reactions.

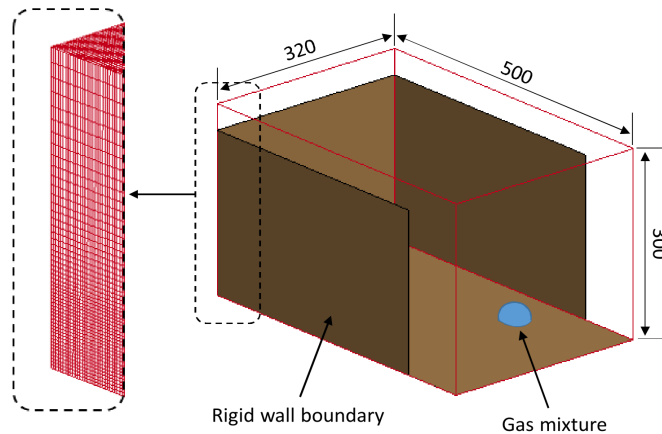


Fig.10: The numerical model (all dimensions are millimeter)

Reaction	Forward rate constant		
	A	n	E
1 H+O2=OH+O	2.60E+14	0.00	16.69
2 H2+O=OH+H	1.80E+10	1.30	8.84
3 H2+OH=H+H2O	2.20E+13	0.00	5.12
4 H+OH+M=H2O+M	2.20E+22	-2.00	0.00
5 CO2+M=CO+O+M	5.50E+21	-1.00	131.8
6 CH4+H=CH3+H2	1.26E+14	0.00	11.92
7 CH4+OH=CH3+H2O	3.47E+03	3.08	1.99
8 CH3+O2=CO+H2O+H	4.08E+13	0.00	29.00
9 CH3+H=CH4	1.00E+12	0.00	0.40
10 C2H6+OH=C2H4+H2O+H	8.71E+09	1.05	1.80
11 C2H4+H=C2H3+H2	1.50E+07	2.00	5.96
12 C2H4+OH=C2H3+H2O	4.80E+12	0.00	1.22
13 C2H3+O2=CO+CO+H+H2	7.94E+14	1.00	31.49
14 C3H8=CH3+C2H4+H	1.70E+16	0.00	84.29

Table 4: Reduced $C_3H_8-O_2$ reaction mechanism, Units are cm^3 , mol, sec, kcal, K, and $k=A T^n \exp(-E/RT)$ (Mawid et al., [17])

Figures 11 to 13 show the variations of pressure versus time for the three assumed sensors, respectively. It can be noted that, although using a smaller element size can greatly improve the accuracy of the results, the accuracy of the results obtained with an element size of 2 mm is acceptable. The direct distance of all three sensors to the blast center is between 235 and 241 millimeters, so the peak over-pressure recorded by all three sensors is expected to be approximately the same. However, as can be seen, the first peak over-pressure recorded by the sensor A is about 1.8 times that of the other two sensors. Due to the proximity of the blast region to the wall 1, a Mach stem is formed that moves along this wall. The formation of this Mach stem will cause higher peak over-pressure on the sensor A than other sensors. This Mach stem causes a peak over-pressure about 0.8 bar at this point. More detail can be found in [4].

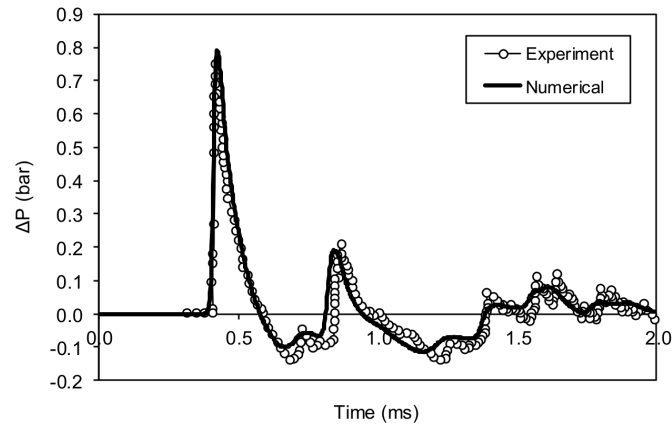


Fig.11: Pressure-time history for sensor A (Walls 1+2+3)

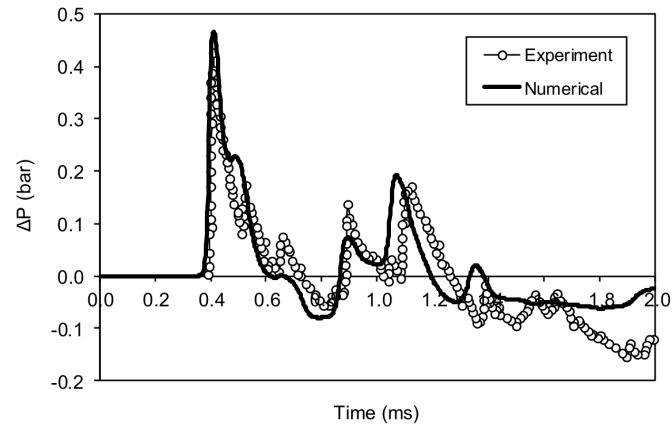


Fig.12: Pressure-time history for sensor B (Walls 1+2+3)

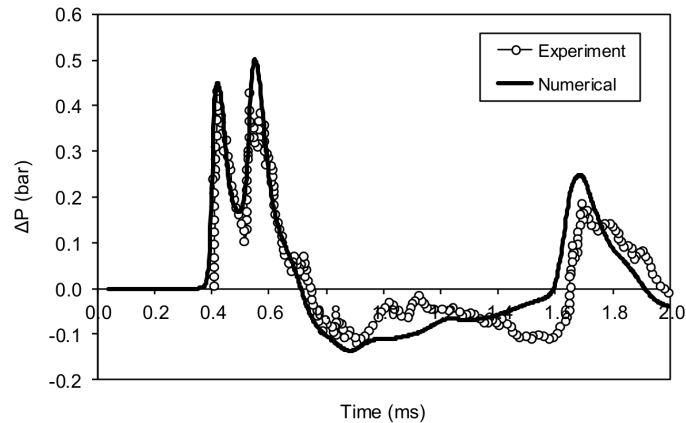


Fig.13: Pressure-time history for sensor C (Walls 1+2+3)

3 FSI using IBM method

To solve FSI problem in compressible fluid, the CESE solver was coupled with the solid mechanics solver in LS-DYNA®. In CESE-IBM FSI solver in LS-DYNA® double precision, the CESE solver was used to solve fluid equations and LS-DYNA® FEM program was used to solve solid structural equations. For the elements near the fluid structure interface, forcing immersed boundary method plus the ghost fluid method were applied [18].

As shown in Figure 14, the fluid solver applies the fluid pressure on the structural elements as external boundary conditions and feedback, with the displacements and velocity of the interface from the structural solver as its new boundary, (UNCLEAR SENTENCE – VERB MISSING ??). More detail of the main steps of this procedure can be found in [18].

To evaluate the accuracy of the CESE-IBM FSI solver with finite rate chemistry model in solving the unsteady FSI problems in reactive compressible flow, three benchmark cases were investigated, and numerical results were compared with the experimental data.

5. Elastic response of aluminum tube to internal H₂-O₂ detonation
6. Gaseous detonation metal-forming
7. Response of concrete barrier wall subjected to hydrogen explosion

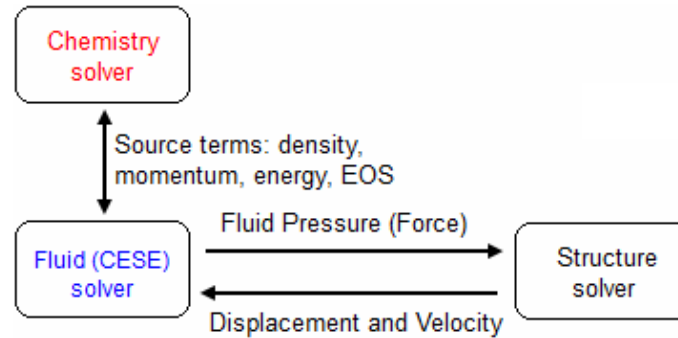


Fig. 14: Diagram with interface coupling data transfer [18]

3.1 Elastic response of aluminum tube to internal H₂-O₂ detonation

In this section, we simulate the Chao experimental test [19] to evaluate the accuracy of detonation wave-structure interaction using CESE-FSI IBM solver. In his work, the elastic response of the tube to the internal detonation of stoichiometric H₂-O₂ mixtures has been investigated. The test tube is made of aluminum 6061-T6 with 41.28 mm outer diameter, 1.5 mm wall thickness, and 1.52 m length. The material properties for the test tube are $\rho=2780$ Kg/m³, $E=69.0$ GPa, and $\nu=0.33$. Figure 15 shows the experimental test set-up. Inside the detonation tube, the flame created by the electric spark accelerates and becomes a detonation wave and propagates into the specimen tube by embedding a Shchelkin spiral. For the measurement of the structure response, five strain gauges were installed at the test tube. The axial locations of these gages from the left end of the tube specimen are 303.8mm, 533.4mm, 762.0mm, 990.6mm and 1219mm, respectively. The initial pressure and temperature of the mixture were 1 bar and 295 K, respectively [19].

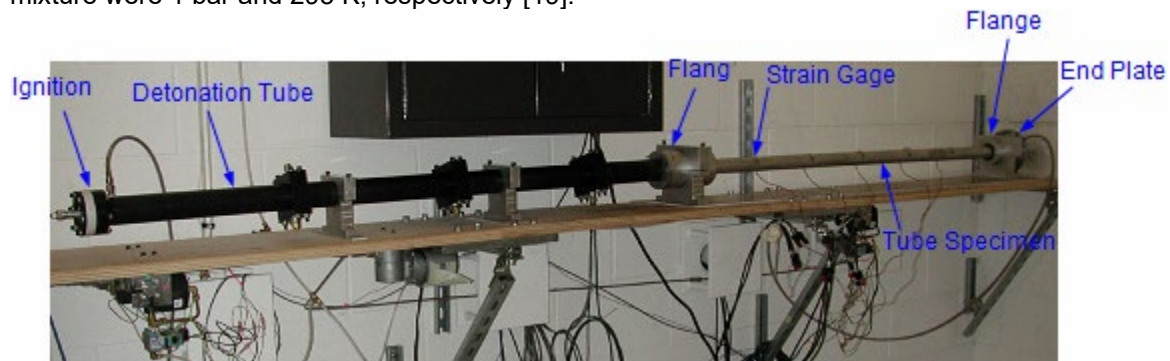


Fig. 15: Tube assembly for detonation experiment apparatus [19]

Figure 16 shows the geometry of the 2D axisymmetric computational set-up. As shown, the mesh of the structure is independent of the fluid mesh. To correctly capture neighboring fluid elements in the FSI algorithm, it is recommended that the structure element size should be larger than the fluid element size [18]. The mesh size of the fluid and structure is 0.5mm and 0.667mm, respectively. In the structural domain at the two ends of the tube, clamping condition is applied. In the fluid domain, the axisymmetric boundary condition applied on the left side. The outflow condition applied on the right side, while the rigid wall boundary conditions are used for the other boundaries.

The detonation of the mixture is accomplished by specifying a high energy initiation region. This region was conceived as a cylindrical shape with 5mm height, containing hot combustion products (e.g., water vapor). The pressure and temperature of this initiation region are considered to 3bar and 3000K, respectively. These initial conditions make the deflagration to detonation transition process very fast.

Similar to the section 2-1, the detailed kinetic mechanism proposed by Liberman et al. [8] was used for H₂-O₂ combustion.

A comparison between numerical results and experiment for all strain gauges are shown in Figure 17. This figure shows the perfect agreement between numerical results and experiments. The effect of the kinetic mechanism on the accuracy of the numerical results is shown in Figure 18. It is observed that the detailed kinetic proposed by CALTECH [15] (8+1 species and 20 reactions) and detailed kinetic proposed by Yungster et al. [11] (8+1 species and 19 reactions) predict the same results. However, the accuracy of these two mechanisms is less than that of the Liberman mechanism (Figure 17). Therefore, the Liberman mechanism is a good choice for H₂-O₂ detonation.

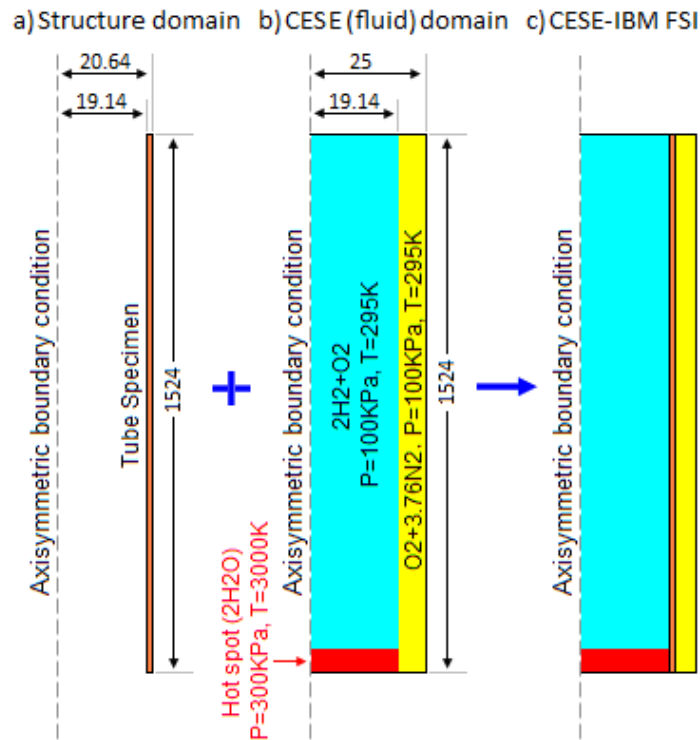


Fig.16: Schematic of the 2D axisymmetric numerical model (all dimensions are in millimeter)

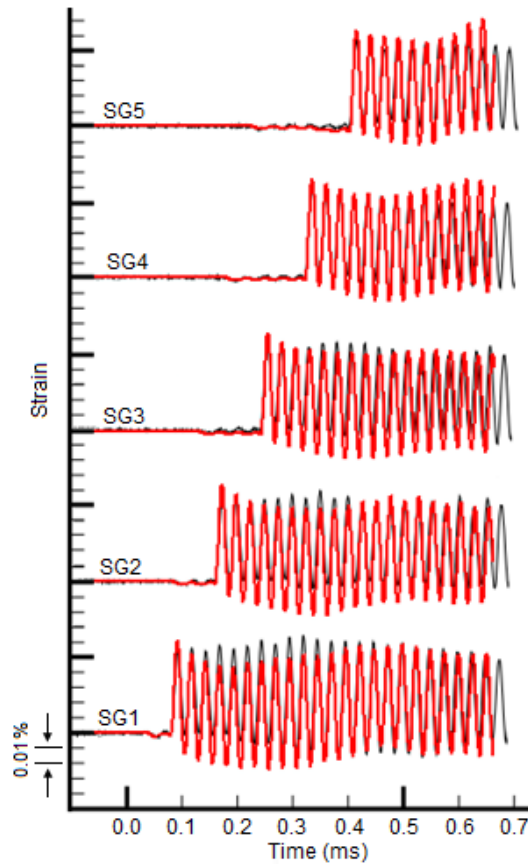


Fig.17: Strain vs. time for strain gauges, (—) present study, (—) experiments [19]

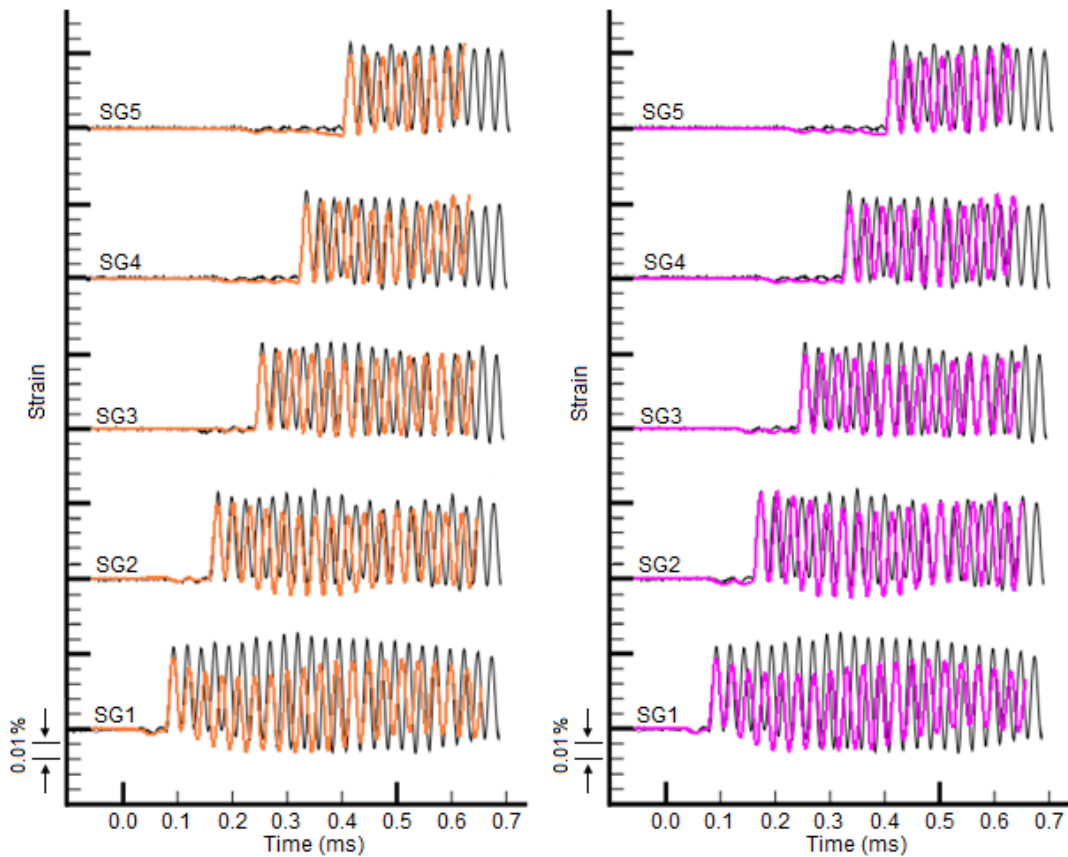


Fig.18: Strain vs. time for strain gauges, (—) CALTECH mechanism [15], (—) Yungster mechanism [11], (—) experiments [19]

3.2 Gaseous detonation metal-forming

To investigate the large deformation of plates caused by gas detonation loading, metal-forming by gaseous detonation in a stoichiometric mixture of H_2-O_2 is simulated and the numerical results are compared with the experimental data. The numerical model is based on the experimental works of Khaleghi et al. [5] for stoichiometric H_2-O_2 mixture and initial pressure of 3bar and initial temperature of 298 K. Also, the die angle was 90 degrees. The schematic of experimental setup is shown in Figure 19. This experimental setup consists of different sections such as a cylindrical combustion chamber made of special seamless steel tube with 210 mm outer diameter, 120 mm inner diameter, 45 mm thickness and 530 mm length, ignition system, Hydrogen and Oxygen cylinders, two valves for controlling the flow of gases and pressure gauges for determining the amounts of pre-detonation pressures. Also, work pieces are circular sheets of mild steel with 1mm thickness and 160 mm diameter.

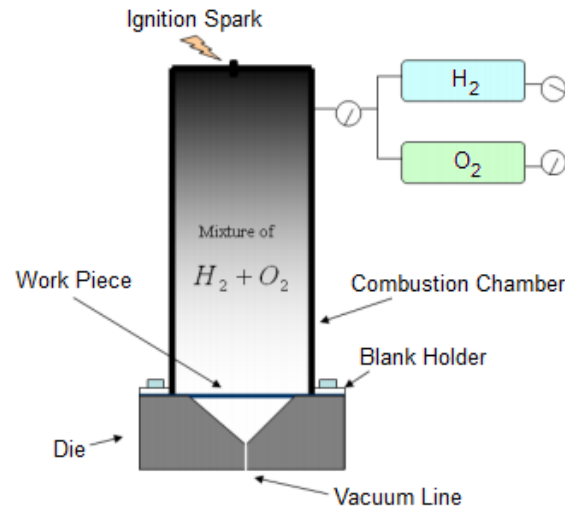


Fig. 19: A conceptual drawing of gas detonation forming apparatus [5]

The 2D axisymmetric of the numerical model is shown in Figure 20. The structural domain is immersed in fluid domain. The element size of CESE fluid domain is 0.25mm, while the element size of the structure is considered 0.50mm.

There is no information about the ignition system in the experiments [5], so we decided to detonate the mixture by specifying an energetic initiation region. This region was considered as a hemispherical shape with 10mm radius containing hot combustion products (e.g., water vapor). The temperature of this initiation region is considered to be 2500K. This initial temperature was considered to be so high to make the DDT process very fast. Similar to the previous section, the detailed kinetic mechanism proposed by Liberman et al. [8] was used for H_2-O_2 combustion. More detail can be found in [6].

Because gaseous detonation metal-forming is a dynamic, high strain rate event, to accurately predict the response of a work piece, high strain rate and material softening due to the increment of adiabatic temperature related to plastic work on the flow stress must be included in the constitutive models. For this reason, we use Johnson-Cook material model, because this material model has been widely used to simulate metal forming [5] and also all required data for structural parts are available in [20-21]. The Johnson-Cook material model parameters for the combustion chamber and work piece are given in Table 5. Here, the materials of both die and combustion chamber are considered to be the same.

The experimental deflection of the center point of the work piece is compared to the numerical results in Figure 21. The numerical results show that the work piece formed completely in 0.60ms after start ignition. Indeed, this figure shows that CESE-IBM FSI method with finite-rate chemistry correctly predicts experimental results of Khaleghi et al. [5].

Gealer et al. [22] experimentally measured the effect of initial pressure on detonation pressure ratio in the stoichiometric mixture of H_2-O_2 . They show that, for initial pressure in range 3 to 5 bar, its ratio would be about eighteen times. According to this, it is expected that, with increase of the initial pressure of the mixture, the work piece deformation will also increase.

The effect of initial pressure of the mixture on the midpoint deflection of work piece calculated here and experimentally measured by [5] are presented in Table 6. It is observed that increasing the initial pressure of the mixture will increase the midpoint deflection of work piece. However, it should be noted that due to the plastic deformation of work piece, the effect of increasing initial pressure of the mixture on deflection of the work piece is not linear.

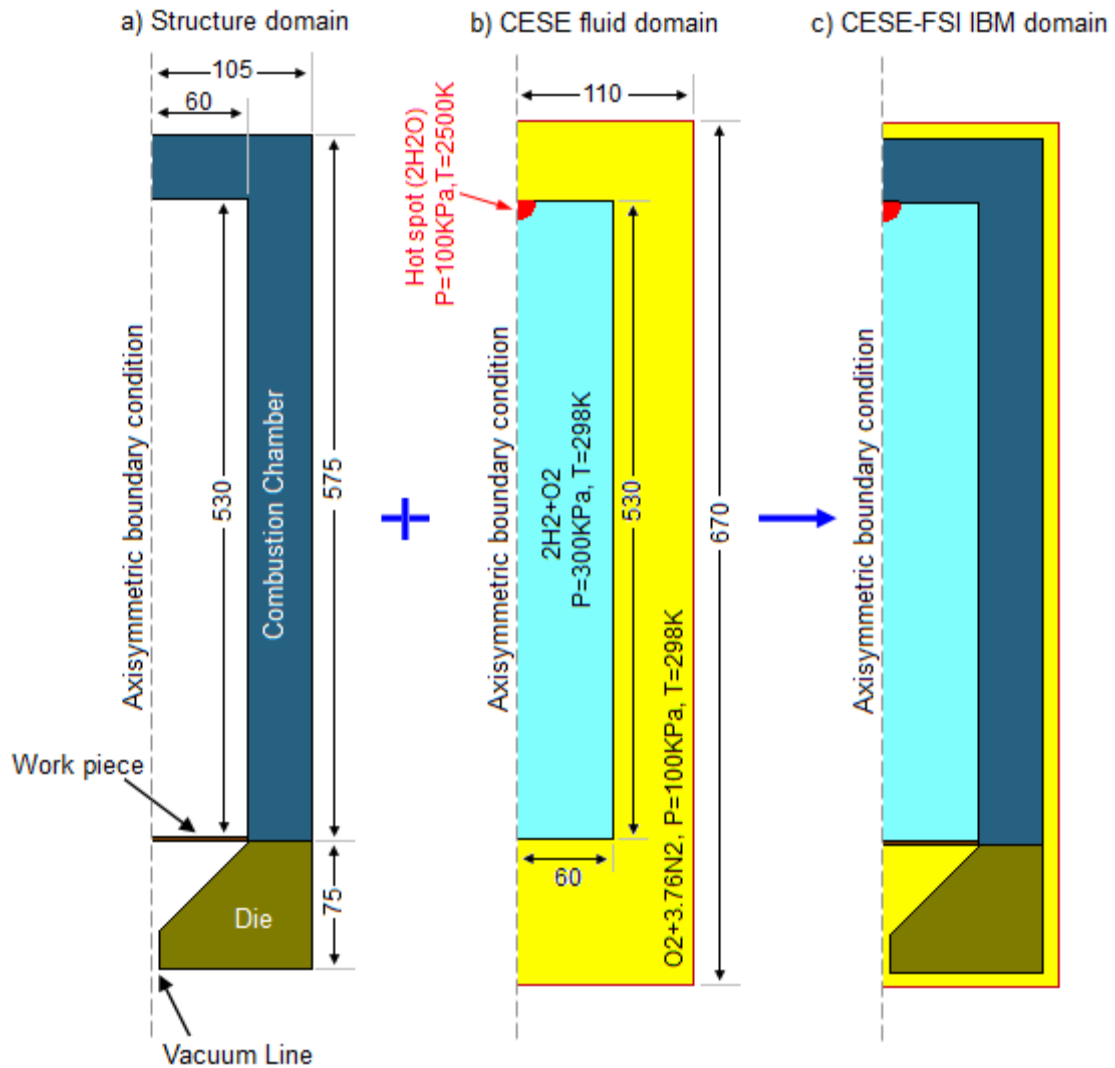


Fig.20: The 2D axisymmetric of the numerical model (all dimensions are millimeter)

Material	A (MPa)	B (MPa)	n	C	m	$\dot{\epsilon}_0$ (S ⁻¹)	Ref.
Mild Steel	217	234	0.643	0.076	1.00	1	[20]
Seamless Steel	792	509	0.260	0.014	1.03	1	[21]

Table 5: The Johnson-Cook parameters

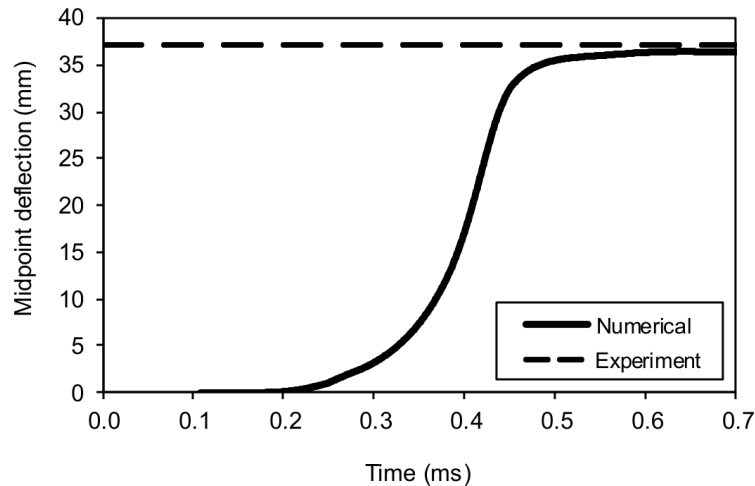


Fig.21: Midpoint deflection of the work piece (experimental and numerical comparison)

P(bar)	Numerical (present)	Experimental [5]
3	36.3	37
4	42.3	48
5	47.5	50

Table 6: Mid-point deflection of work piece (mm)

4 Response of concrete wall subjected to hydrogen explosion

Hydrogen is one of the most promising forms of energy in the next generation. However, hydrogen gas has a strong explode-ability. So, the safety measures on facilities should be established for practical use of hydrogen energy. To investigate the blast-wave characteristics and the response of a concrete wall subjected to the gas explosion load, the explosion of a certain volume of stoichiometric hydrogen/air mixture is simulated and the numerical results are compared with the experimental data [23].

The explosive source was a prismatic 5.27 m³ volume that contained 30% hydrogen and 70% air (stoichiometric mixture). A reinforced concrete wall, 2m tall by 10m wide and 0.15m thick, was set at 4m from the front surface of the source. The unconfined compressive strength of concrete is 48 MPa. The gas mixture was ignited at the bottom center by a high explosive charge. Figure 22 shows the experimental test set-up. The location of pressure transducers and displacement sensor are shown in Figure 23.

The initial pressure and temperature of the mixture were 1 bar and 300 K, respectively. Detonation of the mixture is accomplished by specifying a high energy initiation region. This region is considered as a hemispherical shape. The pressure and temperature of this initiation region are considered to 5 bar and 3000 K, respectively. Figure 24 shows the 3D geometry of the computational set-up. Since the structure geometry and loading are symmetric in one direction, only half of the problem was modeled.

As shown in Figure 24, the rigid wall condition has been applied on the ground, while the outflow condition applied for the other boundaries. Also, the reflective condition applied for symmetric plane. To save computational time, a reduced kinetic proposed by Evans et al. [24], which consist of 6+1 chemical species and 8 reactions was used for hydrogen/air combustion. The reaction mechanism is presented in Table 7.

Figures 25 and 26 show the pressure-time history for sensors on the front and the back of the concrete wall, respectively. It can be noted that, although the accuracy of the numerical results is acceptable, a smaller element size should be used to achieve higher accuracy.

Displacement-time history for sensor on the back of the concrete wall is shown in figure 27. These results showed that the MAT_072R3 (Karagozian & Case (K&C) Concrete Model-Release III) was better able to predict the behavior of concrete under gas explosion.



Fig.22: Experimental test set-up [23]

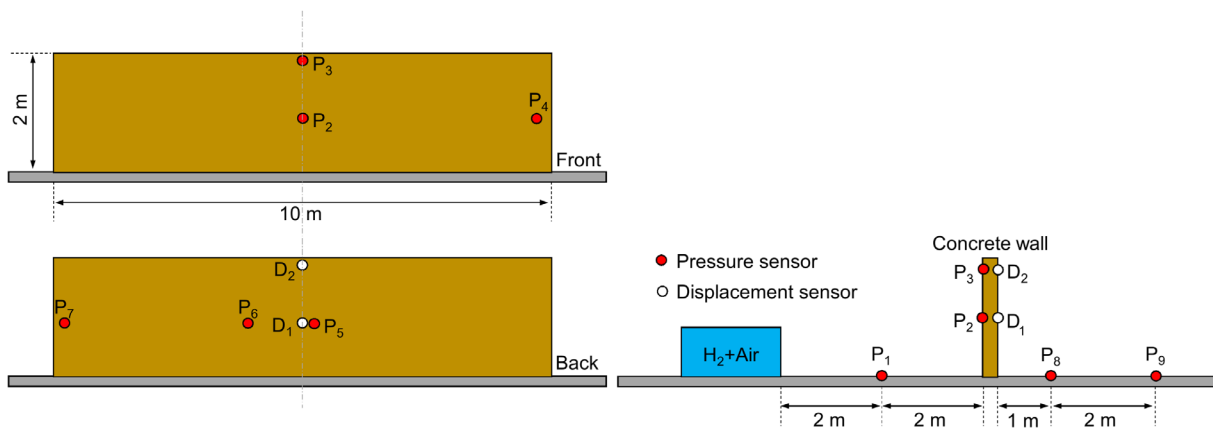


Fig.23: Pressure and displacement sensor locations on the surface of the concrete wall [23]

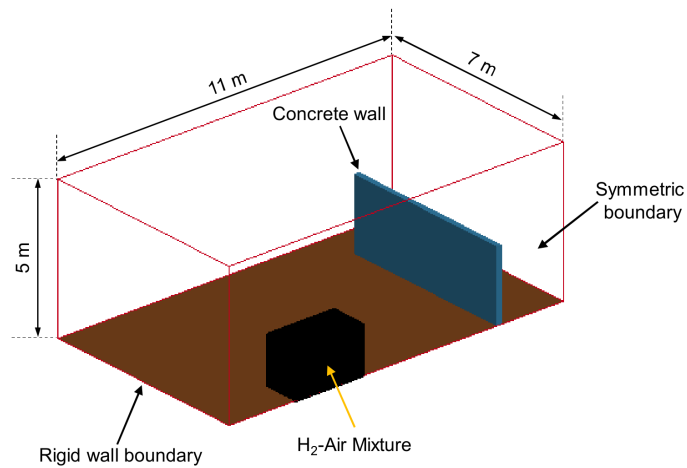


Fig.24: The numerical model

	Reaction	Forward rate constant			Reverse rate constant		
		A	n	E	A	n	E
1	H ₂ +M=H+H+M	5.50E+18	-1.00	103.3	1.8E+18	-1.00	0.0
2	O ₂ +M=O+O+M	7.20E+18	-1.00	117.9	4.0E+17	-1.00	0.0
3	H ₂ O+M=OH+H+M	5.20E+21	-1.50	118.0	4.4E+20	-1.50	0.0
4	OH+M=O+H+M	8.50E+18	-1.00	101.0	7.1E+18	-1.00	0.0
5	H ₂ O+O=OH+OH	5.80E+13	0.00	18.0	5.3E+12	0.00	1.0
6	H ₂ O+H=OH+H ₂	8.40E+13	0.00	20.1	2.0E+13	0.00	5.2
7	O ₂ +H=OH+O	2.20E+14	0.00	16.8	1.5E+13	0.00	0.0
8	H ₂ +O=OH+H	7.50E+13	0.00	11.1	3.0E+13	0.00	8.8

Table 7: Reduced H_2-O_2 reaction mechanism, Units are cm^3 , mol, sec, kcal, K, and $k=A T^n \exp(-E/RT)$ [24]

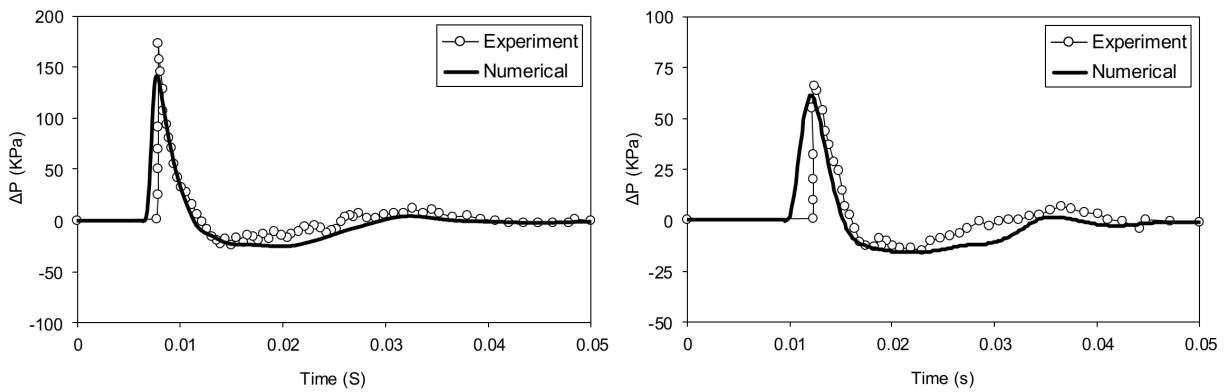


Fig.25: Pressure-time history for sensor on the front of wall (left: P2, right:P4)

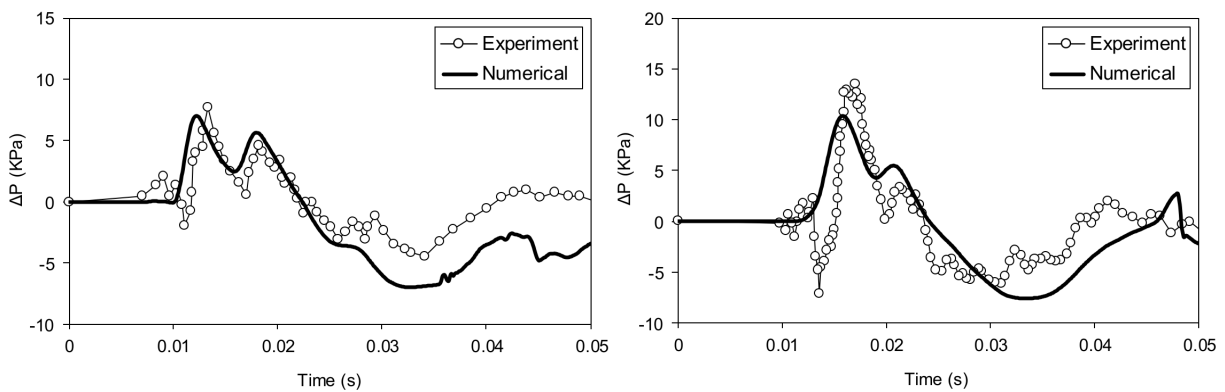


Fig.26: Pressure-time history for sensor on the back of wall (left: P5, right:P7)

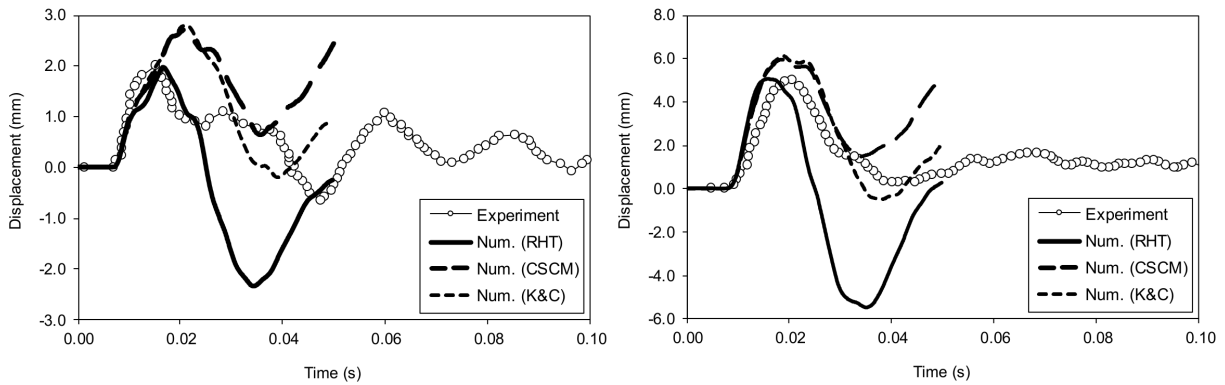


Fig.27: Displacement-time history for sensor on the back of wall (left: D1, right:D2)

5 Summary

In the present paper, with the goal of investigating the accuracy of the CESE solver with finite rate chemistry model, a series of fundamental chemistry problems were simulated using this solver to compare the numerical results with existing experimental data. The comparison between the numerical results and experimental data has shown the high accuracy of the CHEMISTRY solver. But our investigation shows that this accuracy is very dependent on chemical kinetic. Although many chemical kinetic for Hydrogen/Oxygen or Hydrogen/Air combustion have been developed over the years, choosing the appropriate kinetic to solve the desired problem is a great challenge.

For SDT (shock to detonation) problems, the accuracy of the detailed kinetic mechanism proposed by Liberman et al. [8] is greater than the accuracy of the detailed kinetic proposed by CALTECH [15] and Yungster et al. [11]. For $C_3H_8-O_2$ combustion, the reduced kinetic mechanism proposed by Mawid et al. [17] is a good choice.

The good agreement between the numerical results and the experimental data indicates that it is possible to predict the behavior of the blast wave generated by the detonation of a gas mixture in a relatively complex environment accurately by using appropriate chemical kinetics.

It should be noted that, due to access limitations, authors were not able to identify the appropriate kinetic that can accurately estimate the ignition delay time for a hydrogen/oxygen/argon mixture in most cases. It seems that for each case, the appropriate kinetic must be found by trial and error.

6 Literature

- [1] J.E Shepherd, Structural response of piping to internal gas detonation. *J Press Vessel Technol* 131 (2009) 31204.
- [2] H. Rokhy, T. M. Mostofi, 3D numerical simulation of the gas detonation forming of aluminum tubes considering fluid-structure interaction and chemical kinetic model, *Thin-Walled Struct*, 161 (2021), 107469.
- [3] NFPA 68, Standard on explosion protection by deflagration venting; 2007.
- [4] H. Rokhy, H. Soury, Investigation of the confinement effects on the blast wave propagated from gas mixture detonation utilizing the CESE method with finite rate chemistry model, *Combustion Science and Technology* (2021).
- [5] M. Khaleghi, B. S. Aghazadeh, H. Bisadi, Efficient oxyhydrogen mixture determination in gas detonation forming. *International Journal of Mechanical and Mechatronics Engineering*, 7(8) (2013)1748-24.
- [6] H. Rokhy, H. Soury, Fluid structure interaction with a finite rate chemistry model for simulation of gaseous detonation metal-forming, *Int. J. Hydrogen Energy* 44 (2019) 23289 –23302.
- [7] T. R. A. Bussing, G. Pappas, An introduction to pulse detonation engines, AIAA 94-0263
- [8] M. Liberman, M. Ivanov, A. Kiverin, M. Kuznetsov, T. Rakhimova, A. Chukalovskii, On the mechanism of the deflagration-to-detonation transition in a hydrogen-oxygen mixture, *Journal of Experimental and Theoretical Physics*, 111 (2010) 684-698.
- [9] M.P. Moyle, R.B. Morrison, S.W. Churchill, Detonation characteristics of hydrogen-oxygen mixtures, *AIChE Journal*, 6 (1960) 92-96.
- [10] S. Ohyagi, T. Obara, S. Hoshi, P.Cai, T. Yoshihashi, Diffraction and re-initiation of detonations behind a backward-facing step, *Shock Waves* 12 (2002) 221–226.
- [11] S. Yungster, K. Radhakrishnan, Computational and experimental study of NO_x formation in hydrogen-fueled pulse detonation engines, AIAA 2004-3037.
- [12] G.O. Thomas, S.M. Ward, R.LI. Williams, R.J. Bambrey, On critical conditions for detonation initiation by shock reflection from obstacles, *Shock Waves* 12 (2002) 111–119.
- [13] J. D. Anderson, *modern compressible flow*, McGraw Hill Inc., New York, 1982.
- [14] M. O. Connaire, H. J. Curran, J. M. Simmie, W. J Pitz, C. K. Westbrook, A Comprehensive modeling study of hydrogen oxidation, *International journal of chemical kinetics*, 36 (2004) 603-622.
- [15] <http://www.galcit.caltech.edu/EDL/mechanisms/mechs/misc/HydrogenOxygen>
- [16] P. E. Sauvan, I. Sochet, S. Trélat, Analysis of reflected blast wave pressure profiles in a confined room, *Shock Waves*, 22 (2012) 253-264.
- [17] M. A. Mawid, T. W. Park, B. Sekar, C. Arana, Numerical analysis of pulse detonation engine using global and reduced hydrocarbon kinetics, In: 9th AIAA international space planes and hypersonic systems and technologies conference (1999).
- [18] K. S. Im, G. Cook, Z. C. Zhang, S. G. Lee, FSI with detailed chemistry and their applications in LS-DYNA® CESE compressible solver. 11th European LS-DYNA® user conference 2015; Salzburg, Austria
- [19] T. W. Chao, Gaseous Detonation-Driven Fracture of Tubes. PhD thesis; California institute of technology, Pasadena, California USA; 2004
- [20] K. Vedantam, D. Bajaj, N. S. Brar, S. Hill, Johnson-Cook strength models for mild and DP 590 steels. AIP conference proceeding 2006;845,775 .
- [21] G. R. Johnson, W. H. Cook, A constitutive model and data for metals subjected large strains, high strain rates and high temperature, *Proc of the 7th International Symposium on Ballistics* 1983;541-547.
- [22] Gealer RL, Churchill SW. Detonation characteristics of hydrogen-oxygen mixtures at high initial pressure. *AIChE J* 1960; 6(3):501-505.

- [23] T. Nozu, R. Tanaka, T. Ogawa, K. Hibi, Y. Sakai, Numerical Simulation of hydrogen explosion tests with a barrier wall for blast mitigation. In: 1st international conference on hydrogen safety. Pisa, Italy; 2005
- [24] J. S. Evans, C. J. Schexnayder, Influence of chemical kinetics and unmixedness on burning in supersonic hydrogen flames. AIAA J 18(2) (1979) 188-193.